ment. Thieme, Stuttgart, pp 215–219, 1976
16) Garcia-Ibanez E, Garcia-Ibanez JL: Middle fossa vestibular neurectomy: A report of 373 cases. Otolaryngol Head Neck Surg 88: 486–490, 1980
17) Glasscock ME, Kveton JF, Christiansen SG: middle fossa vestibular neurectomy: an update. Otolaryngol Head Neck Surg 92: 216–220, 1984
18) Gavilan J, Gavilan C: Middle fossa vestibular neurectomy: Long-term results. Arch Otolaryngol 110: 785–787, 1984
19) De La Cruz A, McElveen JT Jr: Hearing preservation in vestibular neurectomy. Laryngoscope 94: 874–877, 1984
20) Silverstein H, Norrell H, Haberkamp T: A comparison of retrosigmoid IAC, retrolabyrinthine, and middle fossa vestibular neurectomy for treatment of vertigo. Laryngoscope 97: 165–173, 1987
21) Claassen AJ, Van den Heever CM: Control of Ménière's disease by total vestibular nerve section. South Afr J Surg 25: 152–153, 1987
22) Zini C, Mazzoni A, Gandolfi A, et al.: Retrolabyrinthine versus middle fossa vestibular neurectomy. Am J Otol 9: 448–450, 1988
23) Iurato S, Onofri M: Long-Term Follow-Up after Middle Fossa Vestibular Neurectomy for Ménière's Disease. Ann Otol Rhinol Laryngol 57: 141–147, 1991
24) 北原正章：メニエール病の基礎と臨床（宿題報告）．滋賀医大誌，1981
25) 内藤　泰：メニエール病に適切な外科治療はあるか？—前庭神経切断術による治療の立場から—．JOHNS 21: 1663–1666, 2005

本論文に関しては利益相反に該当する事項はない。

Hindawi Publishing Corporation
Case Reports in Otolaryngology
Volume 2015, Article ID 192764, 3 pages
http://dx.doi.org/10.1155/2015/192764

Hindawi

Case Report

Intractable Persistent Direction-Changing Geotropic Nystagmus Improved by Lateral Semicircular Canal Plugging

Toru Seo, Kazuya Saito, and Katsumi Doi

Department of Otolaryngology, Kinki University Faculty of Medicine, 377-2 Ohno-higashi, Osakasayama, Osaka 589-8511, Japan

Correspondence should be addressed to Toru Seo; tseo@med.kindai.ac.jp

Received 9 September 2014; Revised 1 December 2014; Accepted 15 December 2014

Academic Editor: Dimitrios G. Balatsouras

Antigravitational deviation of the cupula of the lateral semicircular canal, which is also called light cupula, evokes persistent direction-changing geotropic nystagmus with a neutral point. No intractable cases of this condition have been reported. In our case, a 67-year-old man complained of positional vertigo 3 months after developing idiopathic sudden hearing loss in the right ear with vertigo. He showed a persistent direction-changing geotropic nystagmus with a leftward beating nystagmus in the supine position. The nystagmus resolved when his head was turned approximately 30° to the right. He was diagnosed with light cupula of the right lateral semicircular canal and was subsequently treated with an antivertiginous agent. However, his symptoms and positional nystagmus did not improve, so the right lateral semicircular canal was plugged by surgery. One month after surgery, his positional vertigo and nystagmus were completely resolved. We speculated that the cause of the patient's intractable light cupula was an enlarged cupula caused by his idiopathic sudden hearing loss.

1. Introduction

Benign paroxysmal positional vertigo (BPPV) is the most common disorder associated with vertigo. The clinical features of BPPV were first described by Bárány in 1921 [1]. Dix and Hallpike established the clinical concept of the condition in 1952, which remains valid to date [2]. The concept of BPPV has been recently expanded to include a syndrome with positional nystagmus caused by free-floating particles, which may be otoconia detached from the otolith maculae [3]. The features of positional nystagmus depend on the location and status of these particles. When the particles exist freely in the lateral semicircular canal, paroxysmal direction-changing geotropic nystagmus (canalolithiasis type) is evoked, and when the particles adhere to the cupula, persistent direction-changing apogeotropic nystagmus (cupulolithiasis type) is evoked [3].

Shigeno et al. were the first to report cases of persistent direction-changing geotropic nystagmus that could not be explained by the existence of free-floating particles [4]. In these cases, nystagmus was present in the supine position but disappeared when the head was turned 30° to one side (the neutral point). No nystagmus was observed when the horizontal canal was placed on a horizontal plane. All of the features of these cases were identical to those of cupulolithiasis of the lateral semicircular canal, except for the direction of the positional nystagmus. Persistent direction-changing apogeotropic nystagmus in cupulolithiasis generates gravitational deviation of the cupula; thus, it was suggested that the persistent direction-changing geotropic nystagmus was evoked by antigravitational deviation of the cupula in the lateral semicircular canal. Shigeno et al. named this condition light cupula.

The clinical features of positional nystagmus in cases of light cupula have been described by several authors [5–11]. To the best of our knowledge, previously reported cases of positional nystagmus in patients with light cupula have spontaneously resolved within a few days [8–10]. Here, we report the case of a patient with positional nystagmus of the light cupula type that lasted for more than 6 months after the onset of sudden deafness with vertigo; the patient's symptoms were eventually resolved by plugging surgery.

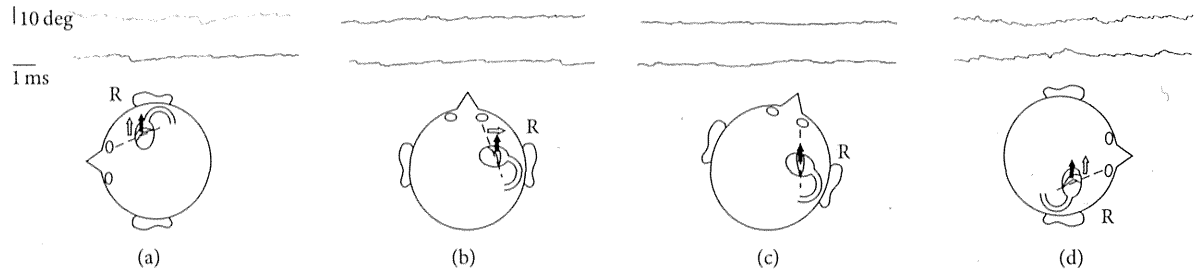

FIGURE 1: Electronystagmogram before surgery. Upper waves indicate eye position since turning head position. Lower waves indicate those one minute after maintaining the head position. The schemas indicate head positions and direction of copular deviations (outlined arrows). Filled arrows indicate direction of antigravitational vector and dotted lines indicate neutral position of cupula. (a) Left side down position. Antigravitational force deviates cupula of the right ear to the ampullofugal direction thus left beating nystagmus was observed. (b) Supine position. As the long axis of cupula is constitutionally out of alignment with anterior-posterior axis, cupula deviates to the ampullofugal direction and left beating nystagmus was also observed. (c) Approximately 30 degrees turn to right position. The long axis of cupula conforms with the antigravitational vector; thus cupula remains stationary and any nystagmus was not observed (neutral point). (d) Right side down position. Antigravitational force deviates cupula to the ampullopetal direction; thus right beating nystagmus was observed.

2. Case Report

A 67-year-old man who suffered from spontaneous vertigo with severe hearing loss in the right ear was diagnosed with idiopathic sudden hearing loss with vertigo and treated with an intravenous steroid by a local otolaryngologist. Although his hearing loss persisted, the patient's vertiginous sensation only lasted for a few days, and subsequent dizziness lasted for a few weeks. Three months after the onset of sudden hearing loss, he complained of a vertiginous sensation when in a right side down position. He was treated with an antivertiginous drug (Difenidol Hydrochloride 75 mg/day) by the local otolaryngologist, but his positional vertigo did not improve. The patient visited our clinic 8 months after the first onset of positional vertigo. He did not have any nystagmus in a sitting position, but a persistent direction-changing geotropic nystagmus was observed (Figure 1). A leftward beating nystagmus was observed when he was in a supine position, and this resolved when his head was turned approximately 30° to the right. A pure tone audiogram revealed high-frequency sensorineural hearing loss in the right ear (Figure 2). Monothermal (20°C) caloric testing revealed severe dysfunction on the right ear (maximum slow phase eye velocity was 26 degrees/second and 3 degrees/second on the left ear and the right ear, resp.). There were no cerebellar findings, and intracranial magnetic resonance imaging did not reveal any abnormal lesions. Based on the features of his nystagmus, he was diagnosed with light cupula of the right lateral semicircular canal. Despite continuous administration of the antivertiginous drug, positional vertigo and nystagmus did not improve. He also had difficulty with activities of daily living owing to the sensation of vertigo. After informed consent was obtained, plugging surgery of the right lateral semicircular canal was performed 11 months after the onset of positional vertigo. The surgical procedure used has been reported previously [10]. He complained of a spontaneous vertiginous sensation for 2 days but did not report any vertiginous sensation 1 month after surgery and was able to perform activities of daily living

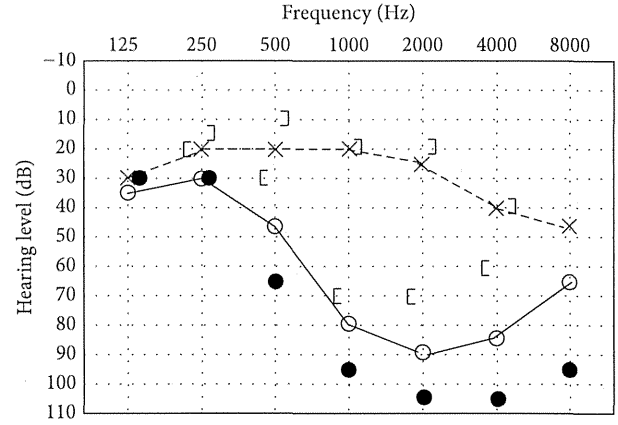

FIGURE 2: Audiogram before and after surgery. Filled circles indicate hearing level in the right ear after surgery.

normally. His audiogram after surgery was not different to that before surgery (Figure 2). Postoperative caloric testing showed no response on the right ear even with ice water stimulation.

3. Discussion

The mechanisms of the antigravitational deviation of the cupula involved in light cupula are controversial. In summary, one mechanism that may be involved is a decrease in mass density due to an increase in ethanol concentration in the cupula after alcohol ingestion [11]. A second potential mechanism is an increased concentration of macromolecules in the endolymph, leading to a decrease in the relative density of the cupula [8, 9]. However, neither of these theories can explain why light cupula occurs in the lateral semicircular canal only [6]. A third potential mechanism is the adherence of light particles to the cupula, similar to the adherence of heavy particles that occurs in cupulolithiasis [8, 9]. The

favorable prognosis of positional nystagmus in cases of light cupula can be explained by detachment of lightweight debris from the cupula. Therefore, most authors agree with this theory.

Our patient experienced positional nystagmus of the light cupula type for more than 6 months; thus, we suspected that the cause of this condition was an irreversible morphological change in the cupula due to preceding idiopathic sudden hearing loss rather than particle adherence. Inagaki et al. suggested that vestibular dysfunction in patients with idiopathic sudden hearing loss originates from morphological changes in the cupula, because the density of vestibular sensory cells is almost normal in cases with vestibular dysfunction [12]. To the best of our knowledge, morphological changes in the cupula have never been reported in studies on the human temporal bone. According to animal models, the cupula shrinks into the inner ear after gentamicin injection and enlarges after disruption of the membranous labyrinth [13, 14]. When the cupula becomes enlarged and the mass remains constant, its relative density should decrease.

Since the top of cupula attaches to the ampullar wall, an occluded semicircular canal creates a closed space between the cupula and the occluded site. Although the space is surrounded by soft tissue as membranous labyrinth and cupula, the animal study confirmed that this space acts as a solid component and inhibits the compression or expansion of the endolymph; therefore the cupula becomes fixed [15, 16]. In other words, successful plugging surgery requires a closed fluid-filled space between the cupula and the occluded site. When the cupula shrinks, the top part detaches from the ampullar wall and a closed space cannot be formed. On the other hand, an enlarged cupula maintains a closed space; thus, plugging surgery can produce successful results. As mentioned above, we speculated that disruption of the membranous labyrinth with idiopathic sudden hearing loss and consequent enlargement of the cupula caused the light cupula type of positional vertigo observed in the current case.

Conflict of Interests

The authors declare that there is no conflict of interests regarding the publication of this paper.

References

[1] E. Bárány, "Diagnose yon Krankheitserscheinungen im Bereiche des Otolithenapparates," *Acta Oto-Laryngologica*, vol. 2, no. 3, pp. 434–437, 1920 (German).

[2] M. R. Dix and C. S. Hallpike, "The pathology, symptomatology and diagnosis of certain common disorders of the vestibular system," *Annals of Otology, Rhinology & Laryngology*, vol. 61, no. 4, pp. 987–1016, 1952.

[3] V. Honrubia, R. W. Baloh, M. R. Harris, and K. M. Jacobson, "Paroxysmal positional vertigo syndrome," *American Journal of Otology*, vol. 20, no. 4, pp. 465–470, 1999.

[4] K. Shigeno, R. Oku, H. Takahashi, H. Kumagami, and S. Nakashima, "Static direction-changing horizontal positional nystagmus of peripheral origin," *Journal of Vestibular Research*, vol. 11, pp. 243–244, 2001-2002.

[5] K. Hiruma and T. Numata, "Positional nystagmus showing neutral points," *ORL*, vol. 66, no. 1, pp. 46–50, 2004.

[6] J. Bergenius and T. Tomanovic, "Persistent geotropic nystagmus—a different kind of cupular pathology and its localizing signs," *Acta Oto-Laryngologica*, vol. 126, no. 7, pp. 698–704, 2006.

[7] K. Hiruma, T. Numata, T. Mitsuhashi, T. Tomemori, R. Watanabe, and Y. Okamoto, "Two types of direction-changing positional nystagmus with neutral points," *Auris Nasus Larynx*, vol. 38, no. 1, pp. 46–51, 2011.

[8] H. Ichijo, "Persistent direction-changing geotropic positional nystagmus," *European Archives of Oto-Rhino-Laryngology*, vol. 269, no. 3, pp. 747–751, 2012.

[9] C.-H. Kim, M.-B. Kim, and J. H. Ban, "Persistent geotropic direction-changing positional nystagmus with a null plane: the light cupula," *Laryngoscope*, vol. 124, no. 1, pp. E15–E19, 2014.

[10] T. Seo, M. Hashimoto, N. Saka, and M. Sakagami, "Hearing and vestibular functions after plugging surgery for the posterior semicircular canal," *Acta Oto-Laryngologica*, vol. 129, no. 11, pp. 1148–1152, 2009.

[11] G. Aschan, "Different types of alcohol nystagmus," *Acta Oto-Laryngologica*, vol. 49, no. s140, pp. 69–78, 1958.

[12] T. Inagaki, S. Cureoglu, N. Morita et al., "Vestibular system changes in sudden deafness with and without vertigo: a human temporal bone study," *Otology and Neurotology*, vol. 33, no. 7, pp. 1151–1155, 2012.

[13] U. Konomi, M. Suzuki, K. Otsuka et al., "Morphological change of the cupula due to an ototoxic agent: a comparison with semicircular canal pathology," *Acta Oto-Laryngologica*, vol. 130, no. 6, pp. 652–658, 2010.

[14] T. Kondo, M. Suzuki, U. Konomi et al., "Changes in the cupula after disruption of the membranous labyrinth," *Acta Oto-Laryngologica*, vol. 132, no. 3, pp. 228–233, 2012.

[15] L. S. Parnes and J. A. McClure, "Posterior semicircular canal occlusion for intractable benign paroxysmal positional vertigo," *Annals of Otology, Rhinology and Laryngology*, vol. 99, no. 5 I, pp. 330–334, 1990.

[16] M. Suzuki, A. Kadir, M. Takamoto, and N. Hayashi, "Experimental model of vertigo induced by detached otoconia," *Acta Oto-Laryngologica*, vol. 116, no. 2, pp. 269–272, 1996.

Acta Oto-Laryngologica. 2014; Early Online, 1–5

informa
healthcare

ORIGINAL ARTICLE

Is a pulling sensation in the anteroposterior direction associated with otolith dysfunction?

NAOKI SAKA[1], TORU SEO[2], SHIGETO OHTA[1] & MASAFUMI SAKAGAMI[1]

[1]*Department of Otolaryngology, Hyogo College of Medicine, Hyogo and* [2]*Department of Otolaryngology, Kinki University Faculty of Medicine, Osaka, Japan*

Abstract

Conclusion: A pulling sensation in the anteroposterior direction is suggested to originate from a dysfunction of the otolith organs. *Objectives:* Previous study with vestibular evoked myogenic potential (VEMP) confirmed that a falling sensation (in an up or down direction) and a lateral tilt sensation (in a right or left direction) were caused by otolith lesions. The purpose of this study was to clarify whether a pulling sensation in the anteroposterior (forward or backward) direction originates from otolith dysfunction. *Methods:* The otolith function was assessed by cervical and ocular VEMPs (cVEMPs and oVEMPs) in 12 patients who complained of a forward or backward pulling sensation. cVEMPs were evaluated by the asymmetry ratio (AR) of the amplitude of the p13-n23 wave and the peak latencies of the p13 and n23 waves. oVEMPs were evaluated by the AR of the amplitude of the n1-p1 wave and the peak latency of the n1 and p1 waves. *Results:* Abnormal ARs on cVEMP were observed in 7 of 12 patients. Nine of 12 patients had abnormal oVEMP results including 3 bilateral absent responses. Most (10 of 12) patients had abnormal cVEMP and/or oVEMP results. The latency of each detected wave was within the normal ranges.

Keywords: *VEMP, otolith organ, saccule, utricle*

Introduction

Caloric testing has been widely used for evaluating inner ear functions in patients with balance problems since it reflects the function of the lateral semicircular canal. Therefore, much is known about vestibular disorders. Rotatory vertigo is the common symptom of patients with canal dysfunction. However, less is known about disequilibrium caused by otolith dysfunction since evaluation of otolith function has previously been difficult. It was suggested that otolith symptoms include a tilting sensation or a sense of moving to and fro, and these are associated with the somatosensory illusion of walking on pillows or on uneven ground [1]. To date, the relationships between such symptoms and otolith function have not been discussed in detail.

Two decades have passed since the first report of vestibular evoked myogenic potential (cervical VEMP, cVEMP) in sternocleidomastoid muscle (SCM) [2]. The origin of the response was confirmed as being the saccular organs in an animal study [3]. Since then, cVEMP testing has become established as an examination for saccular function. More recently, it was reported that the evoked myogenic response was recorded around the eye by bone-conducted vibrations (ocular VEMP, oVEMP) [4]. The origin of oVEMP has been suggested as being the utricular organs [5]. oVEMPs can also be recorded by air-conducted sound stimulation. The amplitudes of oVEMPs to air-conducted sound are also extremely close to those of oVEMPs to bone-conducted vibrations [6]. Thus, measurements of oVEMPs to air-conducted sound have been used for assessing the function of the utricle [7,8]. cVEMP and oVEMP testing can thus now be used for evaluation of the function of both the saccule and utricle.

The most well-known otolith symptom may be Tumarkin's drop attack, which is a sensation of being

Correspondence: Toru Seo, Department of Otolaryngology, Kinki University Faculty of Medicine, 377-2 Ohno-higashi, Osaka-Sayama, Osaka 589-8511, Japan. Tel: +81 72 4366 0221. Fax: +81 72 368 2252. E-mail: tseo@med.kindai.ac.jp

(Received 2 September 2013; accepted 24 October 2013)

ISSN 0001-6489 print/ISSN 1651-2251 online
DOI: 10.3109/00016489.2013.861925

pushed, thrown or knocked to the ground, or the falling sensation in patients with Meniere's disease [9]. These patients frequently have cVEMP abnormalities [10]. Even in patients without Meniere's disease, abnormal cVEMP results were obtained from five of seven patients who experienced a falling sensation [11]. These findings indicate that a falling sensation arises from the sensation of up-and-down movement caused by a dysfunction of the saccule, which senses acceleration in an up-and-down direction (gravity) [12]. On the other hand, oVEMP results were reported to be abnormal in 9 of 10 patients with a lateral tilt sensation [7]. Thus, lateral tilt sensation in a right or left direction is related to a dysfunction of the utricle, which senses acceleration in a right and left direction. The above-mentioned studies indicate that a disequilibrium within linear acceleration arises from a dysfunction in the otolith organs associated with acceleration. The question also arises as to whether a pulling sensation in a forward or backward direction has an otolith origin. The purpose of this study was to find an answer to this question, and so we examined oVEMP and cVEMP testing in patients who complained of a pulling sensation in the anteroposterior direction.

Material and methods

Subjects

Patients who complained of a pulling sensation in either a forward or backward direction and who underwent cVEMP and oVEMP testing were considered candidates for this study. Subjects who had any of the following criteria were excluded: (1) diagnosis of well-known vestibular disorder or other disorders that cause vertigo and/or dizziness; (2) abnormal results from routine examinations conducted at our institution, including primary equilibumetry (gaze, positional, and positioning nystagmus tests, Romberg test, and stepping test), pure tone audiometry, caloric, eye tracking, and optokinetic pattern tests; and (3) cerebellar signs or intracranial lesions detected by brain magnetic resonance imaging.

In total, 12 subjects from our database were enrolled in this study, including 3 males and 9 females who ranged in age from 8 to 59 years (mean 44.7 years). The patient characteristics are shown in Table I.

cVEMP measurement

cVEMP measurements were performed in the usual manner at our institute using a Neuropack Sigma® (Nihon Kohden, Tokyo, Japan) [11]. The active electrodes were placed on the upper half of the SCM muscle, the reference electrode was placed on the upper manubrium sterni, and the ground electrode on the forehead. A tone-burst sound of 135 dB SPL with a frequency of 500 Hz (rise/fall time, 1 ms; plateau time, 4 ms; repetition rate, 5 Hz) was delivered to the ipsilateral ear through a headphone. The evoked myogenic potentials were recorded and averaged 100 times. A bandpass filter from 5 Hz to 1 kHz was used. During the recordings, the subjects lay in a supine position and were instructed to keep their heads rotated to the contralateral side to maintain tonic contraction of the SCM muscle. The average of two runs was used for analysis.

Previous reports have assessed cVEMP results by evaluating the asymmetry ratio (AR) of the p13-n23 amplitude and the peak latencies of the p13 and n23 waves [11]. The ratio was expressed as the percentage difference between the larger and smaller amplitudes, divided by the sum of the two. To define the normal range, 31 healthy volunteers who had neither otological nor neurotological disorders were examined. Their ages ranged from 22 to 59 years (mean 32.7 years). The mean AR was 12.6% (SD, 11.8), and so the normal range was less than 36.3% (mean ± 2 SD). The mean peak latencies of the p13 and n23 waves were 13.6 ms (SD, 1.4) and 22.4 ms (SD, 2.0), respectively. Thus, the normal ranges (mean ± 2 SD) for the p13 and n23 waves were from 10.8 to 16.3 ms, and from 18.4 to 26.4 ms, respectively. When the AR and/or the peak latency extended beyond the normal range, we considered the results to be abnormal.

oVEMP measurements

oVEMPs were measured as described previously using a Neuropack Sigma® [8]. The active electrodes were placed just below the eyelid with the reference electrode 2 cm lower, and the ground electrode was positioned on the forehead. Subjects lay in a supine position and were instructed to maintain a visual fixation point approximately 30° upward during the recording. A tone-burst sound of 135 dB SPL with a frequency of 700 Hz (rise/fall time, 1 ms; plateau time, 4 ms; repetition rate, 5 Hz) was delivered to the contralateral ear through a headphone. Evoked potentials were recorded, and averaged at least 50 times. The bandpass filter was set from 5 Hz to 500 Hz. We defined the initial negative–positive peaks that occurred less than 20 ms after the stimulus as n1 and p1, respectively. To eliminate artifacts, amplitudes smaller than 2 μV were rejected. The average of two runs was used for analysis. Results were also evaluated using the AR of p1-n1 amplitude [8]. This ratio was calculated in the same way as for the cVEMP readings. The mean AR in normal

Table I. Subject characteristics.

Case no.	Age (years)	Sex	Dizziness characterisitcs			cVEMP			oVEMP		
			Trigger	Direction	Duration	Right ear (μV)	Left ear (μV)	Results	Right ear (μV)	Left ear (μV)	Results
1	46	F	Walking	Forward	Few minutes	57	91	Normal	4.1	5.0	Normal
2	56	F	Lying down	Backward	Few minutes	–	259	Abnormal	–	4.4	Abnormal
3	41	F	Walking	Backward	Few minutes	248	140	Normal	10.7	5.0	Abnormal
4	59	F	Lying down	Backward	Few minutes	–	60	Abnormal	–	–	
5	55	M	Riding in a car	Backward	Few minutes	46	–	Abnormal	52.0	12.0	Abnormal
6	40	F	None	Backward	Momentary	250	103	Abnormal	–	–	
7	59	F	Shaking her head	Backward	Momentary	76	98	Normal	5.5	14.6	Abnormal
8	38	F	None	Forward	Few seconds	313	211	Normal	–	–	
9	34	M	None	Backward	Momentary	136	74	Normal	3.7	2.9	Normal
10	57	M	Walking	Backward	Momentary	319	143	Abnormal	10.0	5.0	Abnormal
11	43	F	Getting up	Backward	Few seconds	82	37	Abnormal	2.7	–	Abnormal
12	8	F	Getting up/lying down	Backward	Few seconds	62	28	Abnormal	13.2	8.4	Normal

volunteers was found to be 12.8% (SD, 9.4), and so the normal range was defined as less than 31.6% (mean ± 2 SD). The mean peak latencies of the n1 and p1 waves of the normal volunteers were 10.4 ms (SD, 0.92) and 16.4 ms (SD, 1.1), respectively. Thus, the normal ranges (mean ± 2 SD) for n1 and p1 were from 8.5 to 12.2 ms, and from 14.3 to 18.6 ms, respectively [8]. When the AR and/or the peak latency extended beyond this normal range and when no obvious wave could be obtained from the bilateral ears, we considered the results to be abnormal.

Results

Ten patients complained of a backward pulling sensation and the other two patients complained of a forward pulling sensation (Table I). Some sort of movement triggered episodes of pulling sensations in nine patients. The duration of the episode was less than a few minutes for all patients. Four patients complained of a momentary pulling sensation. None fell down to the ground.

In the cVEMP study, all patients showed responses in at least one ear (Figure 1a). No responses were detected in a unilateral ear in three patients. The peak latencies of the n13 and p23 waves were within the normal range for all detected waves. Abnormal AR results were observed in 7 of the 12 patients.

In the oVEMP study, bilateral responses were absent in three patients. The remaining nine patients showed a distinct wave in at least one ear (Figure 1b). Of these, six patients had abnormal AR results. Therefore, including the patients with bilateral absence, 9 of the 12 patients were considered to have abnormal readings. The peak latencies of the n1 and p1 waves were within the normal ranges for all detected waves.

Ten of the 12 patients had abnormal cVEMP and/or oVEMP results, and 6 patients had abnormal results for both cVEMP and oVEMP.

Discussion

In this study, most (10 of 12) patients who experienced a pulling sensation in the anteroposterior direction had abnormal results on cVEMP and/or oVEMP testing. Abnormal results on oVEMP suggested a disturbance of the utricle and/or the superior vestibular nerve. In the present study, all cases showed normal results on caloric testing, which reflects the function of the superior vestibular nerve. Therefore, the abnormal results of oVEMP indicated utricular dysfunction. Also, abnormal results on cVEMP suggested dysfunction of the saccule and/or the inferior vestibular nerve. The nerve also consisted of the afferent fibers from the posterior semicircular canal, thus abnormal cVEMP results suggest dysfunction of the saccule and/or the posterior canal. Kim et al. reported cases with abnormal results of both head impulse tests on posterior canal and cVEMP [13]. All of their patients complained of spells of vertigo; however, none of our cases did. Thus it was suggested that our case with abnormal cVEMP indicated normal posterior semicircular canal function but saccular dysfunctions.

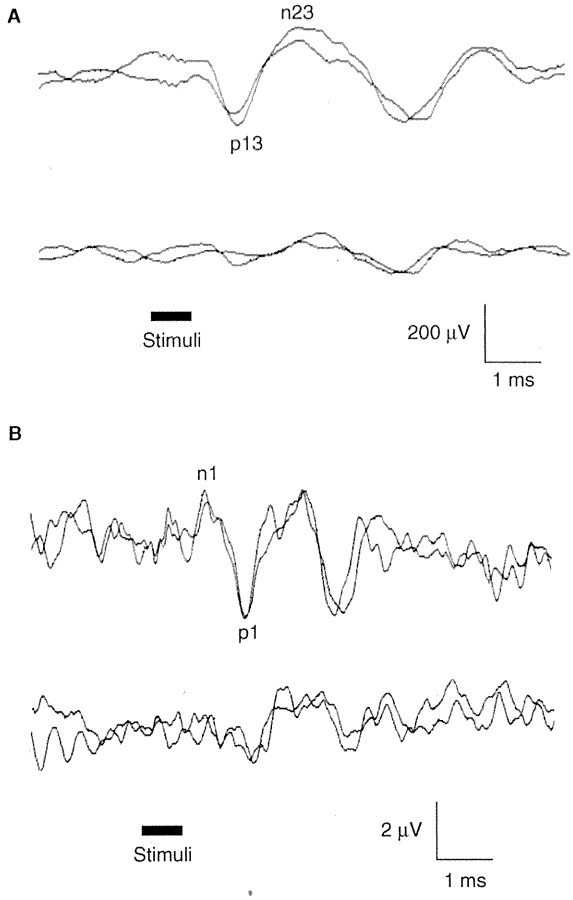

Figure 1. (a) cVEMP and (b) oVEMP results in a 56-year-old female who complained of a pulling sensation in a backward direction when she was lying down. Upper waves represent VEMPs stimulated in the left ear and lower waves represent those in the right ear. Right ear responses were absent for both cVEMP and oVEMP.

As mentioned above, our results strongly suggest that dizziness in the anteroposterior direction originates from saccular and/or utricular dysfunction. The saccular membrane is located almost within the sagittal plane and the utricular membrane is located almost within the horizontal plane; sensory cells respond to linear acceleration within these planes [14]. The anteroposterior axis comprises both the sagittal and horizontal planes, and thus it is responsible for the forward or backward pulling sensation that originates from saccular and/or utricular organs.

Under low intensity of otolith stimulation by linear acceleration, subjects feel the sensation of movement without direction. As the intensity increases, a sensation of linear movement is felt and finally a tilting sensation [14]. Thus, a pulling sensation originates from a certain intensity of stimulation of the otolith. The otolith input reaches the extensor muscles of the lower limbs via the vestibular nuclei and the vestibulospinal tract [15]. Otolith dysfunction may therefore cause leg weakness and continuous falling spells, but none of our series of patients complained of falling. This suggests that the pulling sensation does not originate from a failure of the otolith spinal reflex. Meng et al. reported that vestibulothalamic neurons are activated by otolith stimulation [16], and it is known that stimulation of the thalamus evokes a sensation of motion in humans [17]. We therefore speculate that the pulling sensation detected by VEMP originates from the vestibulothalamic pathway.

In the present study, all patients complained of a pulling sensation that was of short duration. Previous studies have also reported that otolith symptoms only last for a short period (that is, for a few seconds to several minutes, and less than several hours) [7,11]. Ishiyama et al. confirmed damage of the otolith membrane in surgical specimens taken from patients with drop attacks without Meniere's disease [18]. Thus, complete otolith disturbance might result in symptoms of short duration. Why does persistent otolith dysfunction cause short-lasting symptoms? To answer the question, accumulated knowledge about otolith symptoms is required.

What was the etiology of the dysfunction in the otolith organs alone? Seo et al. reported cases with endolymphatic hydrops in the cochlea and the saccule [19]. Schuknecht reported experimental degeneration of otolith membrane by cutting the anterior vestibular artery [20]. We are not sure of the etiology of our cases. To elucidate the answer to this question, accumulation of pathological evidence is required.

Declaration of interest: The authors report no conflicts of interest. The authors alone are responsible for the content and writing of the paper.

References

[1] Creaty MA, Bronstein AM, Brand T, Dieterich M. Neurology of otolith function. Brain 1992;115:647–73.
[2] Colebatch JG, Halmagyi GM. Vestibular evoked potentials in human neck muscles before and after unilateral vestibular deafferentation. Neurology 1992;42:1635–6.
[3] Murofushi T, Curthoys IS, Topple AN, Colebatch JG, Halmagyi GM. Responses of guinea pig primary vestibular neurons to clicks. Exp Brain Res 1995;103:174–8.
[4] Rosengren SM, McAngus Todd NP, Colebatch JG. Vestibular-evoked extraocular potential produced by stimulation with bone-conducted sound. Clin Neurophysiol 2005; 116:1938–48.
[5] Curthoys IS, Kim J, McPhedran SK, Camp AJ. Bone conducted vibration selectively activates irregular primary otolith vestibular neurons in the guinea pig. Exp Brain Res 2006; 175:256–67.

[6] Curthoys IS, Iwasaki S, Chihara Y, Ushio M, McGravie LA, Burgess AM. The ocular vestibular-evoked myogenic potential to air-conducted sound: probable superior vestibular nerve origin. Clin Neurophysiol 2011;122:611–16.
[7] Murofushi T, Nakahara H, Yoshimura E. Assessment of the otolith-ocular reflex using ocular vestibular evoked myogenic potentials in patients with episodic lateral tilt sensation. Neurosci Lett 2012;515:103–6.
[8] Seo T, Saka N, Ohta S, Sakagami M. Detection of utricular dysfunction using ocular vestibular evoked myogenic potential in patients with benign paroxysmal positional vertigo. Neurosci Lett 2013;550:12–16.
[9] Baloh RW, Jacobson K, Winder T. Drop attacks with Menière's syndrome. Ann Neurol 1990;28:384–7.
[10] Timmer FC, Zhou G, Guinan JJ, Kujawa SG, Herrmann BS, Rauch SD. Vestibular evoked myogenic potential (VEMP) in patients with Ménière's disease with drop attacks. Laryngoscope 2006;116:776–9.
[11] Seo T, Miyamoto A, Node M, Sakagami M. Vestibular evoked myogenic potentials of undiagnosed dizziness. Auris Nasus Larynx 2008;35:27–30.
[12] Fernandez C, Goldberg JM. Physiology of peripheral neurons innervating otolith organs of the squirrel monkey. I. Response to static tilts and to long-duration centrifugal force. J Neurophysiol 1976;39:970–84.
[13] Kim JS, Kim HJ. Inferior vestibuar neuritis. J Neurol 2012; 259:1553–60.
[14] Baloh RW, Honrubia V. Central vestibular system. In Baloh RW, Honrubia V, editors. Clinical neurophysiology of the vestibular system. 2nd edn. Philadelphia: FA Davis Co. 1990. p 44–87.
[15] Uchino Y, Kushiro K. Differences between otolith- and semicircular canal-activated neural circuitry in the vestibular system. Neurosci Res 2011;71:315–27.
[16] Meng H, Bai RS, Sato H, Imagawa M, Sasaki M, Uchino Y. Otolith-activated vestibulothalamic neurons in cats. Exp Brain Res 2001;141:415–24.
[17] Hawrylyshyn PA, Rubin AM, Tasker RR, Organ LW, Fredrickson JM. Vestibulothalamic projections in man – a sixth primary sensory pathway. J Neurophysiol 1978;41:394–401.
[18] Ishiyama G, Ishiyama A, Baloh RW. Drop attacks and vertigo secondary to a non-Meniere otologic cause. Arch Neurol 2003;60:71–5.
[19] Seo T, Node M, Miyamoto A, Yukimasa A, Terada T, Sakagami M. Three cases of cochleosaccular endolymphatic hydrops without vertigo revealed by furosemide-loading vestibular evoked myogenic potential test. Otol Neurotol 2003; 24:807–11.
[20] Schuknecht HF. Cupulolothiasis. Arch Otolaryngol 1969;90: 765–78.

Magn Reson Med Sci

TECHNICAL NOTE

E-pub ahead of print by J-STAGE
doi:10.2463/mrms.2014-0065

Imaging of Endolymphatic Hydrops in 10 Minutes: A New Strategy to Reduce Scan Time to One Third

Shinji NAGANAWA[1]*, Hisashi KAWAI[1], Mitsuru IKEDA[2], Michihiko SONE[3], and Tsutomu NAKASHIMA[3]

[1]*Department of Radiology, Nagoya University Graduate School of Medicine*
65 Tsurumai-cho, Shouwa-ku, Nagoya 466–8550, Japan
[2]*Department of Radiological and Medical Laboratory Sciences,*
Nagoya University Graduate School of Medicine
[3]*Department of Otorhinolaryngology, Nagoya University Graduate School of Medicine*
(Received June 10, 2014; Accepted July 16, 2014; published online December 15, 2014)

We measured the size of the endolymph using a newly proposed 10-min magnetic resonance (MR) imaging protocol and compared values with those of the previously reported 31- and 17-min protocols in 15 patients. Values for the 3 protocols did not differ significantly in either the cochlea or vestibule. Correlation among the 3 protocols was strong or relatively strong. Evaluation of endolymphatic hydrops is feasible using the newly proposed 10-min protocol.

Keywords: ***advanced imaging techniques, magnetic resonance imaging, Ménière's disease, temporal bone disease, 3D imaging***

Introduction

The visualization of endolymphatic hydrops was first achieved using a 3-dimensional (3D) fluid attenuated inversion recovery (FLAIR) magnetic resonance (MR) imaging sequence with intratympanic administration of gadolinium-based contrast material (GBCM).[1,2] Recently, heavily T_2-weighted (hT_2W) 3D-FLAIR has been used with the intravenous (IV) administration of a single dose of GBCM (IV-SD-GBCM).[3–5] The generation of a HYDROPS-Mi2 image was proposed (HYbriD of Reversed image Of Positive endolymph signal and native image of positive perilymph Signal-Multiplied by T_2) for easier interpretation of images and semi-quantification of endolymphatic size.[1,6] Generation of that image using the previously reported MR parameters requires 31 min of scan time–14 min for acquisition of an hT_2w 3D-FLAIR or positive perilymph image (PPI),[7] 14 min for acquisition of a positive endolymph image (PEI),[7] and 3 min for acquisition of hT_2W MR cisternography (MRC).[8–11] To shorten the total scan time, generation of another type of image was proposed–a HYDROPS2-Mi2 image (HYbriD of Reversed image Of MR cisternography and a positive Perilymph Signal by heavily T_2-weighted 3D-FLAIR-Multiplied by T_2). This image, generated from PPI (14 min) and MRC (3 min) images, was proposed and tested in comparison with the previous HYDROPS-Mi2 image (acquisition time, 31 min).[1,6] Values of the ratio of endolymphatic area ratio measured on the new image (17 min) correlated well with those measured on the previous type (31 min), and interobserver variability was small.[6] However, the expectation for further reduction of scan time is increasing as the MR evaluation of endolymphatic hydrops is becoming more popular.

We propose an even shorter version of the HYDROPS2-Mi2 to shorten the total scan time further and dramatically, an image generated from a PPI acquired with a reduced number of excitations (NEX, 7 min) and an MRC (3 min) image. In this study, we compared endolymphatic size between HYDROPS-Mi2 (Image A, 31-min acquisition) and HYDROPS2-Mi2 (Image B, 17-min acquisition; Image C, 10-min acquisition) images in patients with clinically suspected endolymphatic hydrops and tested the feasibility of the newly proposed

*Corresponding author, Phone: +81-52-744-2327, Fax: +81-52-744-2335, E-mail: naganawa@med.nagoya-u.ac.jp

10-min protocol (HYDROPS2-Mi2, 10-min acquisition, Image C).

Materials and Methods

Between October and November 2012, 15 patients (4 men, 11 women; aged 25 to 91 years, median 46) underwent MR imaging for the investigation of clinically suspected endolymphatic hydrops. Imaging was begun 4 hours after IV administration of a single dose (0.2 mL/kg or 0.1 mmol/kg body weight) of gadolinium-diethylene-triamine pentaacetic acid-bis methylamide (gadodiamide: Gd-DTPA-BMA; Omniscan, Daiichi-Sankyo Co. Ltd., Tokyo, Japan) on a 3.0-tesla scanner (MAGNETOM® Verio, Siemens, Erlangen, Germany) using a 32-channel array head coil. An experienced otorhinolaryngologist determined the indication for MR imaging based on the presence of ear symptoms, vertigo, average hearing level on pure tone audiometry, results of various ontological tests, and clinical history. The estimated glomerular filtration rate (eGFR) of all patients exceeded 60 mL/min/1.73 m^2.

According to our hospital's clinical protocol for the evaluation of endolymphatic hydrops, all patients underwent hT_2W MRC for anatomical reference of the total lymph fluid, hT_2W 3D-FLAIR with inversion time of 2250 ms (PPI), and hT_2W 3D-IR with inversion time of 2050 ms (PEI).[12] Parameters were set as previously reported.[6] PPI (14 min), PEI (14 min), and MRC (3 min) images and a PPI with reduced NEX (7 min) were obtained. The PPI with reduced NEX (PPI 7 min) was acquired as a back-up for the full PPI (14 min), which might be susceptible to the patient's motion as a result of the lengthy scan time. Table 1 details the scan parameters. The other 3 images, A, B, and C, were generated as follows: Image A (total scan time, 31 min), (PPI − PEI) × MRC; Image B (total scan time, 17 min), (PPI − 0.04 × MRC) × MRC; and Image C (total scan time, 10 min), (PPI 7 min − 0.04 × MRC) × MRC.

The purpose for multiplication of the MRC is to boost the contrast-to-noise ratio between the endo- and perilymph while suppressing and stabilizing the background signal of the bone and air.[13] We employed a constant value of 0.04 according to a recent study.[14] We transferred MR images by CD-ROM to an iMac personal computer (Apple Computer, Inc., Cupertino, CA, USA) with a free DICOM viewer (OsiriX image software, ver. 5.8 32 bit; downloadable at http://www.osirix-viewer.com/index.html), which allowed easy pixel-by-pixel multiplication between the image series in a few seconds.

Pixels with a negative value were estimated as endolymph. In 30 ears, we measured the percentage of the area of endolymphatic space in the total lymphatic space (%EL) for the cochlea and vestibule semi-quantitatively on Images A, B, and C according to the previously reported threshold-based method.[6] A neuroradiologist with 25 years of experience in MR imaging evaluated images.

In brief, the observer manually contoured the cochlea and vestibule separately to set up a region of interest (ROI) on the MRC according to the following instructions:[6]

> "Before starting to contour the cochlea or vestibule on the MRC, set the image window level and width to 400/1000.
>
> "For the cochlear ROI, select the slice on which the cochlear modiolus is visually largest. If the size of the modiolus is comparable on 2 or more slices, choose the slice with the largest height of the modiolus. When contouring the cochlea on the MRC, exclude the modiolus when drawing the ROI.
>
> "For the vestibular ROI, select the lowest slice in which the lateral semicircular canal ring is visualized more than 240°, and exclude the semicircular canal and ampulla when drawing the ROI for the vestibule on the MRC."

The ROI of the cochlear slice was defined to select the middle part of the cochlea, and the ROI of the vestibular slice, the middle of the vestibule. These ROIs drawn on the MRC were copied and pasted onto Images A, B, and C. We used the histogram function of OsiriX to measure the number of all pixels within the ROI and the number of pixels with a negative signal intensity value (i.e., endolymph) within the ROI.

The ratio of the area (%) of endolymphatic space in the entire lymphatic space (%EL) was defined as: %EL = (the number of negative pixels for the endolymph in the ROI divided by the total number of pixels in the ROI) × 100. We compared the measured %EL values among Images A, B and C and evaluated the correlation between %EL values in the 2 pairs of processed images by a Pearson's correlation coefficient (r). A linear regression line was found by implicit function fitting with an orthogonal distance regression iteration algorithm. We evaluated differences between the %EL values in the 2 pairs of processed images using a paired t-test

Table 1. Pulse sequence parameters

Sequence name	Type	Repetition time (ms)	Echo time (ms)	Inversion time (ms)	Flip angle (degrees)	Section thickness (mm)	Pixel size (mm)	Number of slices	Echo train length	Field of view (mm)	Matrix size	Number of excitations	Scan time (min)	Bandwidth (Hz/pixel)
MR cisternography (MRC)	SPACE with restore pulse	4400	544	NA	90/ initial 180 decrease to constant 120	1	0.5 × 0.5	104	173	150 × 180	322 × 384	1.8	3	434
Heavily T_2 weighted 3D-FLAIR (PPI)	SPACE with inversion pulse	9000	544	2250	90/ initial 180 decrease to constant 120	1	0.5 × 0.5	104	173	150 × 180	322 × 384	2 or 4	7 or 14	434
Heavily T_2 weighted 3D-inversion recovery (PEI)	SPACE with inversion pulse	9000	544	2050	90/initial 180 decrease to constant 120	1	0.5 × 0.5	104	173	150 × 180	322 × 384	2	7	434

Generalized autocalibrating partially parallel acquisitions (GRAPPA) × 2 for all sequences
FLAIR, fluid attenuated inversion recovery; PEI, positive endolymph image; PPI, positive perilymph image; SPACE, sampling perfection with application-optimized contrasts using different flip angle evolutions
All sequences utilize frequency selective fat suppression pre-pulse.
Each 3-dimensional (3D) slab is set in an identical axial orientation and has 104 slices.

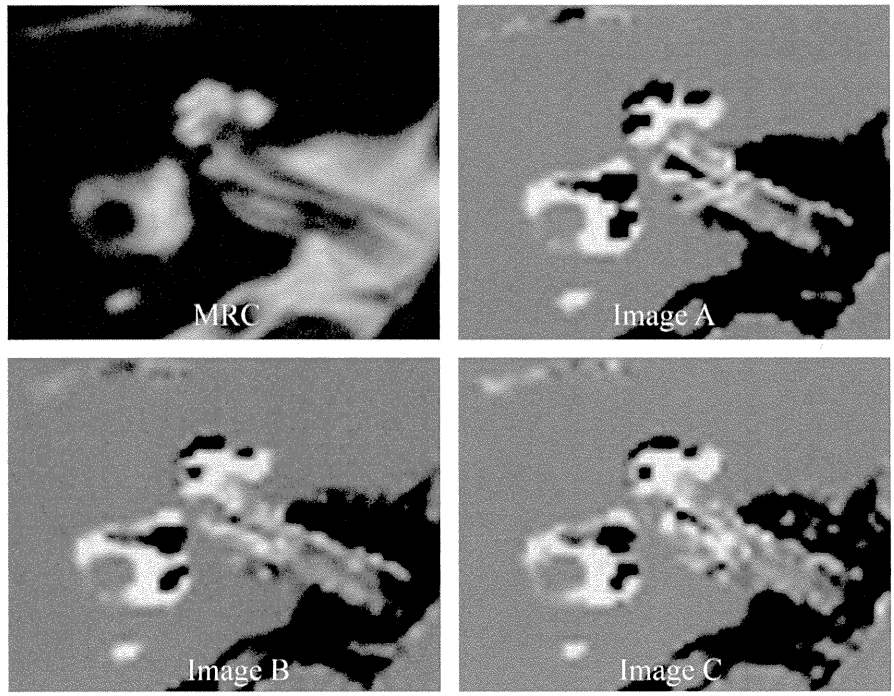

Fig. 1. Representative images from a 50-year-old man with right fluctuating hearing loss without vertigo. Magnetic resonance cisternography (MRC) demonstrates the total space of lymphatic fluid as a bright signal. Image A is a HYDROPS-Mi2 image (HYbriD of Reversed image Of Positive endolymph signal and native image of positive perilymph Signal-Multiplied by T_2) generated from 3 kinds of image data and obtained in a total scan time of 31 min. Images B and C are HYDROPS2-Mi2 images (HYbriD of Reversed image Of MR cisternography and a positive Perilymph Signal by heavily T_2-weighted 3D-FLAIR-Multiplied by T_2). Image B is generated from 2 kinds of image data obtained with a total scan time of 17 min, whereas Image C is generated from 2 kinds of image data obtained with a total scan time of 10 min. In Images A, B, and C, the black areas in the cochlea and vestibule are estimated as endolymph, and the white areas are estimated as perilymph. In this particular ear, significant endolymphatic hydrops is seen in the cochlea but not in the vestibule in all Images A, B, and C.

with Bonferroni corrections for multiple comparisons at a significance level of 5%.

The medical ethics committee of our institution approved this retrospective study, and informed consent was waived.

Results

All patients underwent MR scanning without significant motion. In all patients, Images A, B and C allowed separate visualization of the endo- and perilymph (Fig. 1). The MRC showed the total lymph space anatomy.

Table 2 lists the mean %EL values of the cochlea and vestibule in each image; the values did not differ significantly among Images A, B and C both in cochlea and vestibule.

Figure 2 shows the relationship between the %EL in the 2 pairs of processed cochlear and vestibular

Table 2. Mean values of the %EL of the cochlea and vestibule in each image

		mean %EL	Standard deviation
Cochlea	Image A	26.7	22.9
	Image B	24.9	16.9
	Image C	28.1	17.5
Vestibule	Image A	38.1	31.8
	Image B	37.5	29.1
	Image C	37.3	27.4

No significant difference between Images A, B, and C in both the cochlea and vestibule
%EL = (number of negative pixels for the endolymph in the region of interest [ROI] divided by the total number of pixels in the ROI) × 100

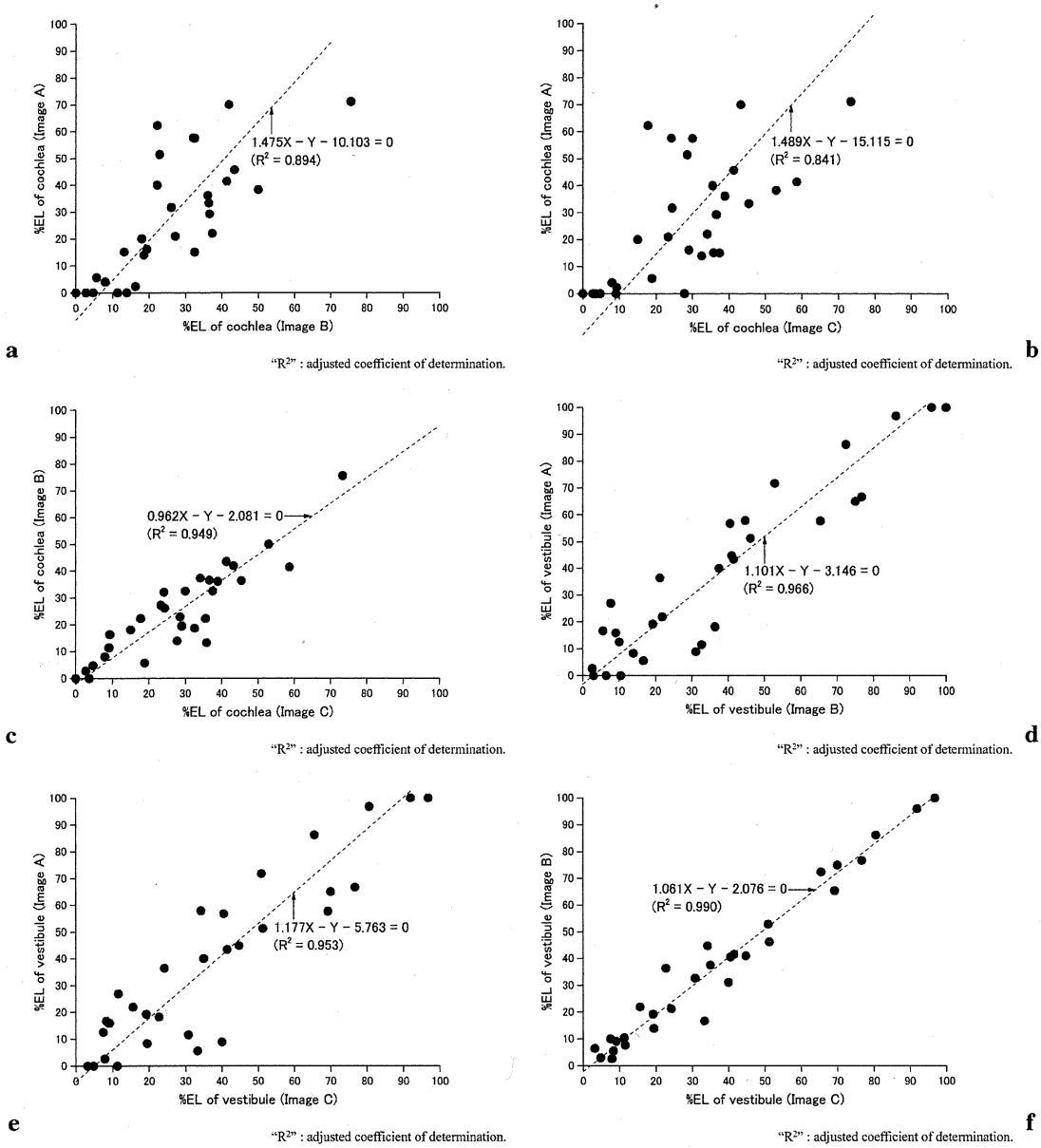

Fig. 2. Scattergrams of values of the ratio of the area of endolymphatic space in the entire lymphatic space (%EL) for the cochlea and vestibule between the 2 processed images. "R^2" indicates the adjusted coefficient of determination. Note that this value of R is not the same value as the Pearson's correlation coefficient. Linear regression lines are found by implicit function fitting with an orthogonal distance regression iteration algorithm. (**a**) Correlation of the %EL between Images A and B in the cochlea. Note that some data points of Image A show values of 0. (**b**) Correlation of the %EL between Images A and C in the cochlea. Note that some data points of Image A show values of 0. (**c**) Correlation of the %EL between Images B and C in the cochlea. Note that the correlation is strong between Images B and C. (**d**) Correlation of the %EL between Images A and B in the vestibule. Note that some data points of Image A show values of 0. (**e**) Correlation of the %EL between Images A and C in the vestibule. Note that some data points of Image A show values of 0. (**f**) Correlation of the %EL between Images B and C in the vestibule. Note that the correlation is strong between Images B and C.

images. A strong or relatively strong linear correlation was observed between them in the cochlear images; the Pearson' correlation coefficient (r) was 0.772 between Images A and B, 0.655 between Image A and C, and 0.901 between Images B and C ($P < 0.001$, for all). A strong linear correlation was also observed between the vestibular images; the Pearson' correlation coefficient (r) was 0.934 between Images A and B, 0.906 between Images A and C, and 0.980 between Images B and C ($P <$

0.001, for all). Except between Images A and B and between Images A and C of the cochlea, the slope of the estimated linear regression line was close to one.

Discussion

A comparison between Images A and B reported previously using different patient groups showed strong linear correlation of the %EL values between the images in both the cochlea and vestibule.[6] The Pearson correlation coefficients between Images A and B by 3 observers ranged from 0.734 to 0.9 in the cochlea and from 0.924 to 0.933 in the vestibule. No significant difference in the %EL values between observers was noted. In the present study, the correlation coefficients between Images A and B, 0.772 in the cochlea and 0.934 in the vestibule, were similar to those reported in the previous study. These similar findings in a different patient cohort add further reliability to the semi-quantitative measurement method by Images A and B.

In the current study, we observed strong or relatively strong linear correlations between Images A and C and between Images B and C in both the cochlea and vestibule. In particular, we observed a strong linear correlation between Images B and C in both the cochlea ($r = 0.901$) and vestibule ($r = 0.980$). These results might be expected because the only difference between Images B and C was the number of excitations used for acquisition (i.e., signal-to-noise ratio [SNR]). Thus, Image C can be used instead of Image B. A protocol with fewer excitations is thought to suffer from a lower SNR, but the %EL values correlated well with those obtained by the protocol with longer scan time. This is probably due to compensation in the SNR by multiplication of the MRC. A shorter scan time reduces the chance of image degradation from patient motion. Furthermore, a protocol with shorter scan time can be fit more easily into a busy clinical scanner schedule.

Some data points of Image A showed zero values in either the cochlea or vestibule (Fig. 2). Even in a healthy condition, there is some endolymph in the labyrinth. Image A might be underestimating the %EL values in lower values.

The lack of a standard of reference for values of EL percentage is a limitation of this study, so we cannot determine which values are nearest the real values. However, the results of the present study might be valuable for the conversion of some data from one method to those of another method. Such combination of data obtained by different imaging protocols would promote a larger scale study.

Conclusions

The newly proposed 10-min protocol (HYDROPS2-Mi2; Image C) might be feasible for the measurement of endolymphatic size after IV-SD-GD. This option will promote more widespread use of MR imaging evaluation of endolymphatic hydrops by clinicians.

Acknowledgements

This study was supported by grants-in-aid for scientific research from the Japanese Society for the Promotion of Science (JSPS KAKENHI, numbers 25293263 and 24659562) to S.N.

References

1. Naganawa S, Nakashima T. Visualization of endolymphatic hydrops with MR imaging in patients with Ménière's disease and related pathologies: current status of its methods and clinical significance. Jpn J Radiol 2014; 32:191–204.
2. Nakashima T, Naganawa S, Sugiura M, et al. Visualization of endolymphatic hydrops in patients with Meniere's disease. Laryngoscope 2007; 117:415–420.
3. Naganawa S, Yamazaki M, Kawai H, Bokura K, Sone M, Nakashima T. Visualization of endolymphatic hydrops in Ménière's disease with single-dose intravenous gadolinium-based contrast media using heavily T(2)-weighted 3D-FLAIR. Magn Reson Med Sci 2010; 9:237–242.
4. Naganawa S, Yamazaki M, Kawai H, Bokura K, Sone M, Nakashima T. Visualization of endolymphatic hydrops in Ménière's disease after single-dose intravenous gadolinium-based contrast medium: timing of optimal enhancement. Magn Reson Med Sci 2012; 11:43–51.
5. Naganawa S, Yamazaki M, Kawai H, Bokura K, Sone M, Nakashima T. Visualization of endolymphatic hydrops in Ménière's disease after intravenous administration of single-dose gadodiamide at 1.5T. Magn Reson Med Sci 2013; 12:137–139.
6. Naganawa S, Suzuki K, Nakamichi R, et al. Semiquantification of endolymphatic size on MR imaging after intravenous injection of single-dose gadodiamide: comparison between two types of processing strategies. Magn Reson Med Sci 2013; 12:261–269.
7. Naganawa S, Yamazaki M, Kawai H, Bokura K, Sone M, Nakashima T. Imaging of endolymphatic and perilymphatic fluid after intravenous administration of single-dose gadodiamide. Magn Reson Med Sci 2012; 11:145–150.
8. Naganawa S, Itoh T, Fukatsu H, et al. Three-dimensional fast spin-echo MR of the inner ear: ultra-long echo train length and half-Fourier technique. AJNR Am J Neuroradiol 1998; 19:739–741.

9. Naganawa S, Koshikawa T, Fukatsu H, Ishigaki T, Aoki I, Ninomiya A. Fast recovery 3D fast spin-echo MR imaging of the inner ear at 3 T. AJNR Am J Neuroradiol 2002; 23:299–302.
10. Naganawa S, Koshikawa T, Fukatsu H, Ishigaki T, Fukuta T. MR cisternography of the cerebellopontine angle: comparison of three-dimensional fast asymmetrical spin-echo and three-dimensional constructive interference in the steady-state sequences. AJNR Am J Neuroradiol 2001; 22:1179–1185.
11. Nakamura T, Naganawa S, Koshikawa T, et al. High-spatial-resolution MR cisternography of the cerebellopontine angle in 90 seconds with a zero-fill interpolated fast recovery 3D fast asymmetric spin-echo sequence. AJNR Am J Neuroradiol 2002; 23:1407–1412.
12. Naganawa S, Sugiura M, Kawamura M, Fukatsu H, Sone M, Nakashima T. Imaging of endolymphatic and perilymphatic fluid at 3T after intratympanic administration of gadolinium-diethylene-triamine pentaacetic acid. AJNR Am J Neuroradiol 2008; 29: 724–726.
13. Naganawa S, Yamazaki M, Kawai H, Bokura K, Sone M, Nakashima T. Imaging of Ménière's disease after intravenous administration of single-dose gadodiamide: utility of multiplication of MR cisternography and HYDROPS image. Magn Reson Med Sci 2013; 12:63–68.
14. Naganawa S, Suzuki K, Yamazaki M, Sakurai Y, Ikeda M. Time course for measuring endolymphatic size in healthy volunteers following intravenous administration of gadoteridol. Magn Reson Med Sci 2014; 13:73–80.

Magn Reson Med Sci

MAJOR PAPER

E-pub ahead of print by J-STAGE
doi:10.2463/mrms.2013-0080

Time Course for Measuring Endolymphatic Size in Healthy Volunteers Following Intravenous Administration of Gadoteridol

Shinji NAGANAWA[1]*, Kojiro SUZUKI[1], Masahiro YAMAZAKI[1], Yasuo SAKURAI[1], and Mitsuru IKEDA[2]

[1]*Department of Radiology, Nagoya University Graduate School of Medicine 65 Tsurumai-cho, Shouwa-ku, Nagoya 466–8550, Japan*
[2]*Department of Radiological and Medical Laboratory Sciences, Nagoya University Graduate School of Medicine*

(Received August 7, 2013; Accepted October 30, 2013; published online April 28, 2014)

Purpose: We developed semi-quantitative methods to measure endolymphatic size on images obtained 4 hours after intravenous administration of single-dose gadolinium-based contrast medium (IV-SD-GBCM) and found little variation in results between observers. We used the methods to measure the size of the endolymph in healthy volunteers at various times after IV-SD-GBCM and attempted to determine the optimal timing for the evaluation.

Methods: In 8 healthy male volunteers, we obtained heavily T_2-weighted 3-dimensional fluid-attenuated inversion recovery (hT_2W-3D-FLAIR) images 1.5, 3, 4.5, and 6 hours after IV-SD-GBCM as positive perilymph images (PPI) as well as acquiring positive endolymph images (PEI) and magnetic resonance cisternography (MRC). To evaluate the endolymph, we generated 2 kinds of processed images (HYDROPS-Mi2 and HYDROPS2-Mi2) by subtracting PEI or MRC from PPI as previously proposed. We semi-quantitatively measured the ratio of the area of the endolymph (%EL) to that of total lymph on the 2 kinds of generated images for the cochlea and vestibule according to the previously proposed method. We analyzed statistics to evaluate the change in %EL over time and used analysis of variance (ANOVA) for a 2×4 repeated-measures design to assess difference in image type. We adopted 5% as a significance level.

Results: The %EL was significantly larger at 1.5 hours after IV-SD-GBCM than at 3, 4.5, and 6 hours in both the cochlea and vestibule for both kinds of generated images. Between 4.5 and 6 hours, the %EL plateaued for both the cochlea and vestibule, and the 2 kinds of generated images did not differ significantly.

Conclusion: A delay of 1.5 hours after IV-SD-GBCM is not sufficient to evaluate endolymphatic size. The %EL plateaus between 4.5 and 6 hours. These data might be valuable for further clinical studies.

Keywords: ***advanced imaging techniques, endolymphatic hydrops, magnetic resonance imaging, 3D imaging***

Introduction

Intratympanic (IT) administration of gadolinium-based contrast media (GBCM) using 3-dimensional fluid-attenuated inversion recovery (3D-FLAIR) has enabled visualization of endolymphatic hydrops in patients with Ménière's disease.[1] As well, the higher sensitivity of heavily T_2-weighted 3D-FLAIR (hT_2W-3D-FLAIR) sequences to low concentrations of GBCM has permitted visualization of endolymphatic hydrops using intravenous administration (IV) of GBCM.[1–3] In both methods, GBCM is distributed mainly in the perilymph and not the endolymph. The endolymphatic space is recognized as the area filled with fluid in which

*Corresponding author, Phone: +81-52-744-2327, Fax: +81-52-744-2335, E-mail: naganawa@med.nagoya-u.ac.jp

Table. Pulse sequence parameters

Sequence name	Type	Repetition time (ms)	Echo time (ms)	Inversion time (ms)	Flip angle (degrees)	Section thickness (mm)	Pixel size (mm)	Number of slices	Echo train length	Field of view (mm)	Matrix size	Number of excitations	Scan time (min)
MR cisternography (MRC)	SPACE with restore pulse	4400	544	NA	90/initial 180 decrease to constant 120	1	0.5 × 0.5	104	173	150 × 180	322 × 384	1.8	3
Heavily T_2-weighted 3D-FLAIR (PPI)	SPACE with inversion pulse	9000	544	2250	90/initial 180 decrease to constant 120	1	0.5 × 0.5	104	173	150 × 180	322 × 384	2	7
Heavily T_2-weighted 3D inversion recovery (PEI)	SPACE with inversion pulse	9000	544	2050	90/initial 180 decrease to constant 120	1	0.5 × 0.5	104	173	150 × 180	322 × 384	2	7

GRAPPA × 2 for all sequences
3D, 3-dimensional; FLAIR, fluid-attenuated inversion recovery; GRAPPA, generalized autocalibrating partially parallel acquisitions; NA, not applicable;
PEI, positive endolymph image; PPI, positive perilymph image; SPACE, sampling perfection with application-optimized contrasts using different flip angle evolutions
All sequences utilize frequency selective fat suppression prepulse, and MRC utilizes restore magnetization pulse at the end of the echo train.
Each 3D slab is set in an identical axial orientation.

there is no GBCM distribution.[4–7] Although the IT administration of GBCM is an off-label use and requires puncture of the tympanic membrane, various institutions have employed this method.[8–14] On the other hand, recent studies of the relationship between the degree of endolymphatic hydrops and patient symptoms have used the IV administration of single-dose GBCM (IV-SD-GBCM).[15–17] A previous study in volunteers set the time delay after IV-SD-GBCM at around 4 hours,[18] and a significant rise in perilymph signal beginning 1.5 hours after IV-SD-GBCM in volunteers has been reported.[19] The latter report also showed plateauing of the perilymph signal from 3 to 6 hours after IV-SD-GBCM. However, endolymphatic size over time after IV-SD-GBCM has not been investigated.

Semi-quantitative methods for evaluating the size of the endolymphatic space on images obtained 4 hours after IV-SD-GBCM have been proposed, and results of their use in patients with Ménière's disease have varied little between observers.[20]

The purpose of the current study was to measure the size of the endolymphatic space in healthy volunteers at various time points after IV-SD-GBCM using the proposed semiquantitative methods and to determine the optimal timing for evaluating the endolymphatic space.

Materials and Methods

The medical ethics committee of our institution approved this study of healthy volunteers, and written informed consent was obtained from all participants.

Subjects

Subjects were 8 healthy male volunteers aged 29 to 53 years (median 37 years) with no history of hearing loss, vertigo, cranial disease, head trauma, renal disease, or heart disease who took no daily medications.

MR imaging

All MR imaging was performed on a 3-tesla scanner (Verio, Siemens, Erlangen, Germany) using a 32-channel array head coil. All volunteers underwent heavily T_2-weighted magnetic resonance cisternography (MRC) for anatomical reference of the fluid space and hT_2W-3D-FLAIR (positive perilymph image: PPI) with inversion time of 2250 ms according to the clinical protocol of our hospital for evaluating endolymphatic hydrops.[19–21] We also obtained a positive endolymph image (PEI) with a shorter inversion time (TI) of 2050 ms.[22]

We set parameters as previously reported.[22,23]

Table details scan parameters. All MRC, PPI, and PEI acquisitions employed an identical field of view, matrix size, and slice thickness to facilitate comparisons. Sets of MRC, PPI, and PEI images were obtained before and at 0.5, 1.5, 3, 4.5, and 6 hours after IV-SD-GBCM.

After the pre-contrast scan, subjects received a single dose (0.2 mL/kg body weight or 0.1 mmol/kg body weight) of gadoteridol (Gd-HP-DO3A: ProHance, Eisai, Tokyo, Japan) by IV administration, after which they were permitted to exit the magnet room and rest during the interval between MR scans without instructions to restrict behavior.

Image processing

Before measuring endolymphatic size, we preprocessed images. On the scanner console, we generated HYDROPS (HYbriD of Reversed image Of Positive endolymph signal and native image of positive perilymph Signal) images by subtracting PEI from PPI,[23] and we generated HYDROPS2 (HYbriD of Reversed image Of MR cisternography and positive Perilymph Signal by heavily T_2-weighted 3D-FLAIR)[24] images by subtracting MRC multiplied by a constant value of 0.04 from PPI.

The signal intensity values of the perilymph are usually far larger on MRC without inversion pulse than on PPI with inversion pulse, and we determined that this constant value would reduce the original signal intensity value of the perilymph on PPI to approximately half the original value after subtracting the MRC multiplied by the constant value. Before generating HYDROPS2 images, we measured the signal intensity values of the perilymph in the vestibule on PPI and MRC at 4.5 hours in 4 ears of the initial 2 volunteers, drawing a circular region of interest (ROI) on the scanner console to set a constant value to balance the signal intensity values between the PPI and MRC. Based on the results, we determined an average constant value of 0.04.

For the result of subtraction, we allowed negative signal values for both HYDROPS and HYDROPS2 images. Acquisition of source images takes 14 minutes for HYDROPS and 10 minutes for HYDROPS2. In this study, we applied no image motion registration program during subtraction. For the HYDROPS and HYDROPS2 images, a neuroradiologist subjectively confirmed the absence of misregistration artifact, i.e., apparent double contour of the labyrinth.

HYDROPS, HYDROPS2, and MRC images were transferred by CD-ROM to an iMac personal computer (Apple Computer, Inc., Cupertino, CA, USA) with a free DICOM viewer (OsiriX image software, ver. 5.6, 32 bit; downloadable at: http://www.osirix-viewer.com/index.html), which allowed easy pixel-by-pixel multiplication between image series in a few seconds.

We obtained a HYDROPS-Mi2 (HYDROPS image Multiplied with heavily T_2-weighted MR cisternography, Image ♯1 in the present study) image by multiplying the MRC and HYDROPS.[21]

We obtained a HYDROPS2-Mi2 (HYDROPS2 image Multiplied with heavily T_2-weighted MR cisternography, Image ♯2 in the present study) image by multiplying the MRC and HYDROPS2.[20]

Our aim in multiplying MRC onto HYDROPS and HYDROPS2 images was to set to zero the signal intensity value of bony structures possibly included in the ROI (i.e., osseous spiral lamina, interscalar septum, and bony wall of the labyrinth). Without multiplication, such bony structures might show non-zero negative signal intensity value because of the low signal-to-noise ratio of HYDROPS and HYDROPS2, which would result in the overestimation of the size of the area of the endolymph.

Acquisition of source images takes 17 min for HYDROPS-Mi2 images and 10 min for HYDROPS2-Mi2 images.

We performed semi-quantitative analysis of endolymphatic size using these HYDROPS-Mi2 (Image ♯1) and HYDROPS2-Mi2 (Image ♯2) images according to the previously reported method.[20]

Image analysis

A neuroradiologist with 24 years of experience in the field of clinical MR imaging semi-quantitatively evaluated images in 16 ears of 8 volunteers. We separately measured endolymphatic size for the cochlea and vestibule according to previously reported methods.

In brief, the image window level and width were set to 400/1000 before contouring of the cochlea or vestibule on the MRC at each time point. The ROI for the cochlea was drawn on the slice on which the cochlear modiolus is visually largest or on the slice with the largest height of the modiolus if the modiolus is of comparable size on 2 or more slices. When contouring the cochlea on MRC, the POI should be drawn to exclude the modiolus.

The ROI for the vestibule should be drawn on the lowest slice on which the lateral semicircular canal ring is visualized more than 240° and should exclude the semicircular canal and ampulla when the ROI for the vestibule is drawn on MRC.[20]

We defined the ROI of the slice of the cochlea to include the middle part of the cochlea and that of the slice of the vestibule to include the middle